Available online at www.sciencedirect.com

ScienceDirect

Mendeleev Commun., 2024, **34**, 100–103

Mendeleev Communications

Probing of microgel–enzyme films on graphite substrates by means of atomic force microscopy and amperometry

Larisa V. Sigolaeva,* Olga V. Efremova and Dmitry V. Pergushov

Department of Chemistry, M. V. Lomonosov Moscow State University, 119991 Moscow, Russian Federation. E-mail: lsigolaeva@belozersky.msu.ru

DOI: 10.1016/j.mencom.2024.01.030

Microgel–enzyme coatings were fabricated onto graphite substrates (highly oriented pyrolytic graphite or graphite-based screen-printed electrodes) *via* two-stage sequential procedure, which consists in adsorption of a pH- and temperature-sensitive copolymer microgel, followed by electrostatic immobilization of glucose oxidase into the microgel film. The microgel–enzyme coatings were examined by means of atomic force microscopy showing remarkable coverage of graphite surface by the microgels and visualizing the immobilized enzyme. Finally, amperometry was applied to reveal the effect of the polymeric (microgel) matrix on temperature behavior of glucose oxidase in the microgel–enzyme coatings.

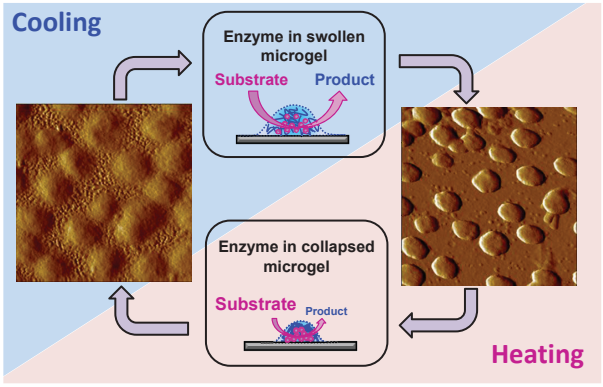

Keywords: microgel, stimuli-sensitivity, poly(*N*-isopropylacrylamide-*co*-*N*-(3-aminopropyl)methacrylamide), enzyme immobilization, enzymatic response regulation, glucose oxidase.

Gentle immobilization of enzymes is one of the most important challenges in biotechnology and related areas as the immobilized enzymes are extensively exploited in pharmaceutical and biofuel production, food processing, waste-water treatment, and biosensors.[1,2] In many cases, this can be realized with polymers,[3] which due to numerous binding sites can act as capacious hosts for biomolecules. Polymeric hydrogels are perfect and most suitable matrices for immobilization of enzymes as they contain a large amount of water, thereby providing favorable (highly hydrated) microenvironment for biomolecules and preserving their biological activity.[4]

In this context, stimuli-sensitive microgels,[5–9] that is, hydrogels whose particles have a size in the (sub)micron range (typically, 50 nm to 5 μm), are nowadays of considerable interest. They respond to variations in one (or many) physical, chemical, or biochemical stimuli,[5–9] and this makes such polymers very promising for biocatalytic applications.[10] Recently, we have highlighted application of a pH- and temperature sensitive cationic microgel based on poly(*N*-isopropylacrylamide) (PNIPAM) for efficient immobilization of enzymes and engineering of microgel–enzyme systems (films),[11–16] wherein activity of the immobilized enzyme is regulated by temperature.[17] In this work, we reveal main morphological features of the microgel and microgel–enzyme films by means of atomic force microscopy (AFM) and with the use of an electrochemical technique (amperometry) examine temperature dependence of activity of the enzyme immobilized into the microgel films.

The copolymer microgel — hereinafter referred to as P(NIPAM-*co*-APMA) microgel — was synthesized *via* precipitation polymerization of *N*-isopropylacrylamide (NIPAM) and a cationic comonomer *N*-(3-aminopropyl)methacrylamide (APMA) in the presence of a cross-linker *N*,*N*′-methylene bisacrylamide as described elsewhere.[14] The content of NIPAM, APMA, and the cross-linker in the reaction mixture were about 92, 3 and 5 mol%, respectively. As was shown for the sample with a higher content of the cationic comonomer (APMA) units, the microgel is fully charged (protonated) at pH 5.2, while it becomes fully uncharged (deprotonated) at pH 10.3.[14] Temperature sensitivity of the P(NIPAM-*co*-APMA) microgel is manifested by a remarkable change of its hydrodynamic size (measured by means of dynamic light scattering in water), which decreases from R_h = 148 ± 2 nm at 20 °C to 83 ± 2 nm at 50 °C, where R_h is hydrodynamic radius of the microgel. The volume phase transition temperature (VPTT) for P(NIPAM-*co*-APMA) microgel was determined by dynamic light scattering in water to be about 36 °C, which is close to VPTT of 32 °C reported for the pure PNIPAM.[18]

Being adsorbed at pH 9.5 onto a hydrophobic surface – highly oriented pyrolytic graphite (HOPG) –, the P(NIPAM-*co*-APMA) microgel forms a nearly continuous coating, wherein single well-distinguishable microgel particles are located very close to each other as follows from the height and amplitude AFM images of the microgel films taken in a semicontact mode in a dry state [Figure 1(*a*),(*e*)]. Thus, the AFM imaging confirms remarkable modification of the HOPG surface by the P(NIPAM-*co*-APMA) microgel even at low temperature and at the pH where its particles are not fully deprotonated. Their topographic features (height and lateral diameter) presented in Table 1 suggest rather strong deformation of the P(NIPAM-*co*-APMA) microgel upon adsorption, although the measured microgel's height is also affected by the catilever's tip upon scanning. This is in line with

our previous data[11,15] reported for another cationic PNIPAM-based microgel and also with other reports.[19–24]

Further, such microgel films when brought to pH 7 can bind enzymes bearing the opposite charge.[11–17] In this work, glucose oxidase (GOx) from *Aspergillus niger* (MW = 160 kDa, E.C. 1.1.3.4, activity 168 100 U g^{-1} of solid) was taken as a model enzyme because of a low isoelectric point (pI = 4.2). Successful binding of GOx to the P(NIPAM-*co*-APMA) microgel films is evident from the 3D-height AFM images [Figure 1(*b*)] but is pronouncedly manifested in the highly detailed AFM images obtained when changes of the amplitude signal are registered [Figures 1(*f*)]. Indeed, numerous small round-shaped objects (with the size of about 10 nm) are found in-between the adsorbed microgel particles. Obviously, these are globules of GOx, which are immobilized *via* the electrostatic binding onto the P(NIPAM-*co*-APMA) microgel. Apparently, one can see only the outer enzyme globules located on the periphery of the microgel (presumably, bound to the dangling chains) although their considerable amount is thought to be bound inside the P(NIPAM-*co*-APMA) microgel particles and cannot be visualized. A comparison of the topographic features (height and lateral diameter) of the intact microgels *vs.* the GOx-loaded ones shows some increase of the object diameter for the latter ones but without any notable changes in their height (Table 1, *cf.* Sample 1 and Sample 2).

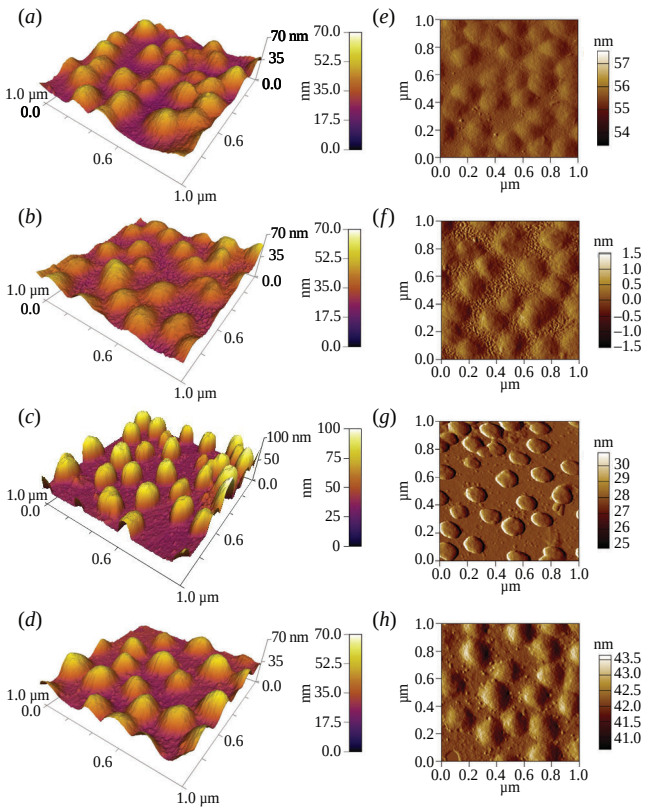

Figure 1 The 3D-height (*a*)–(*d*) and the high detailed amplitude (*e*)–(*h*) AFM images for the P(NIPAM-*co*-APMA) microgel film (*a*),(*e*), the P(NIPAM-*co*-APMA)/GOx microgel–enzyme film (*b*),(*f*), the P(NIPAM-*co*-APMA)/GOx microgel–enzyme film after incubation at 50 °C (pH 7.5) for 60 min (*c*),(*g*); and the P(NIPAM-*co*-APMA)/GOx microgel–enzyme film after incubation at 50 °C (pH 7.5) for 60 min and then incubation at 25 °C (pH 7.5) for 60 min (*d*),(*h*). The P(NIPAM-*co*-APMA) microgel was adsorbed at 25 °C from 1 g dm^{-3} solutions in 10 mM Tris buffer of pH 9.5 for 60 min onto HOPG and then the microgel film was gently washed with Milli-Q water. The enzyme was loaded into the P(NIPAM-*co*-APMA) microgel film at pH 7 and 25 °C using 10^{-5} M solution of GOx in 10 mM Tris buffer of pH 7 for 40 min, followed by gentle washing of the microgel–enzyme film with Milli-Q water. The AFM images were taken in the semicontact mode in the dry state.

Table 1 Comparative topographic features of the P(NIPAM-*co*-APMA) microgel and the P(NIPAM-*co*-APMA)/GOx microgel–enzyme films on HOPG.

Sample no.	Description	Adsorption/ Treatment	Object height/ nm[a]	Object diameter/ nm[a,b]	Number of objects per 5×5 μm scan
1	Microgel	Adsorption of the microgel for 60 min at pH 9.5, 25 °C	19 ± 3 (*n* = 51)	211 ± 21 (*n* = 51)	735 ± 25
2	Microgel/ GOx	Sample 1 after loading with GOx for 40 min at pH 7, 25 °C	17 ± 3 (*n* = 47)	238 ± 22 (*n* = 47)	707 ± 66
3	Microgel/ GOx	Sample 2 after incubation for 60 min at pH 7.5, 50 °C	41 ± 6 (*n* = 49)	126 ± 15 (*n* = 49)	691 ± 35
4	Microgel/ GOx	Sample 3 after incubation for 60 min at pH 7.5, 25 °C	21 ± 3 (*n* = 28)	225 ± 16 (*n* = 28)	693 ± 29

[a] Mean ± SD, calculated for *n* objects. [b] No tip convolution was taken into account.

We further examined the effect of temperature on the behavior of the microgel–enzyme assemblies at the HOPG surface. The adsorbed P(NIPAM-*co*-APMA) microgel was found to retain its thermosensitivity even if it is loaded with GOx. This clearly follows from the AFM images of the microgel–enzyme film, which was subsequently brought to the high (50 °C > VPTT) and low (25 °C < VPTT) temperatures when the microgel transformed from the swollen state to the collapsed one and back. The 3D-height and highly detailed amplitude AFM images as well as the topographic features of the microgel–enzyme assemblies are also given in Figure 1(*c*),(*d*),(*g*),(*h*) and Table 1 (Samples 3 and 4). Indeed, the P(NIPAM-*co*-APMA) microgel loaded with GOx appears as strongly deformed round-shaped objects [Figure 1(*b*),(*f*)] with a mean height of 17 ± 3 nm and a mean lateral diameter of 238 ± 22 nm (Table 1, Sample 2). Upon a prolonged (60 min) heating at 50 °C, the microgel–enzyme assemblies are transformed to higher and less flattened ones [Figure 1(*c*),(*g*)] with a height of 41 ± 6 nm and a lateral diameter of 126 ± 15 nm (Table 1, Sample 3). Cooling back to 25 °C results in a nearly complete restoring the initial shape of the microgel–enzyme assemblies as follows from Figure 1(*d*),(*h*) and Table 1 (Sample 4). It is worth noting that the total amount of microgel particles counted in the AFM images remains nearly unchanged at any stage of the temperature treatment (Table 1), thereby confirming the strong interaction of the P(NIPAM-*co*-APMA) microgel with the HOPG surface and indicates no microgel desorption. At the same time, one can note a certain decrease in the number of the small (10 nm) objects (the enzyme globules) bound to the dangling chains of the microgels for Sample 4 [*cf.* Figures 1(*f*) and 1(*h*)]. This might be a result of a partial release of GOx from the microgel film upon the temperature up-and-down changes.

To understand the enzymatic behavior of GOx immobilized into the adsorbed P(NIPAM-*co*-APMA) microgels, amperometric measurements were applied. The electrochemically active microgel–enzyme constructs were prepared as follows. First, the microgels were adsorbed in their considerably hydrophobized state (at 50 °C and pH 9.5) onto the graphite-based screen-printed electrodes, which were modified by a thin layer of manganese dioxide nanoparticles to impart the electrodes sensitivity to hydrogen peroxide.[25] Afterwards, GOx

was loaded into the microgel films at 25 °C and pH 7 due to the electrostatic interaction of the negatively charged enzyme with the positively charged microgel film as already demonstrated.[11–17] The enzymatic responses of the immobilized GOx were measured by recording the oxidative current in response to addition of β-D-glucose at an applied potential of +450 mV *versus* Ag/AgCl [15–17] (for details see Figure S1 in Online Supplementary Materials).

Figure 2 shows a temperature dependence of the enzymatic responses of the microgel–enzyme constructs in the Arrhenius' coordinates, which exhibits a clear breaking point. Indeed, the responses linearly increase with temperature in the low-temperature range, while there is a distinct decrease of the responses with temperature when it exceeds a certain value (T_{bp} = 36.6 °C). We attribute such a behavior to a temperature-induced transition of the microgel from the swollen state to the collapsed one, which could decrease the accessibility of the GOx's active site for the substrate. It is worth noting that the volume phase transition of the P(NIPAM-*co*-APMA) microgel as revealed by dynamic light scattering (see above) is observed in the same temperature range (VPTT = 36 °C). For the P(NIPAM-*co*-APMA) microgel used in this study, the effect of the collapse of the polymer (microgel) matrix is much more pronounced compared to the one with the higher content of the cationic comonomer (APMA) units,[14] which can be associated to a stronger temperature sensitivity with the decreasing charge of the microgel. We should emphasize that native GOx does not demonstrate any deviations from linearity in the Arrhenius plot as was examined by independent spectrophotometric technique (see Figure S2).

Finally, the enzymatic responses of the immobilized GOx were measured in a multiple cyclic mode by cycling temperature as follows 25 °C → T_{bp} → 50 °C → T_{bp}→ 25 °C. From Figure 3, one can see that at $T > T_{bp}$ in each temperature cycle they demonstrate no further increase. Actually, the enzymatic responses are remained almost at the level of ones at T_{bp}, which is in contrast to what is observed for the mode when temperature gradually increases (*cf*. Figures 2 and 3). With the exception of the first cycle, they go down to the initial values upon lowering temperature to 25 °C. Starting from the second cycle, the enzymatic responses at given temperature appear to demonstrate only a weak trend to decrease with the rising number of repetitions (cycles). All these findings strongly suggest that the enzymatic activity of GOx immobilized into such microgel films can be (reversibly) regulated by variations in temperature.

It should be noted that the initial enzymatic response at 25 °C (first cycle) is notably higher than those in the following cycles at the same temperature. This could be explained by a release of a certain fraction of GOx from the adsorbed P(NIPAM-*co*-APMA) microgel upon temperature changes, which also follows from the results obtained by means of AFM (Figure 1). The same explanation can be given for a further (starting from a second cycle) weak lowering of the corresponding enzymatic responses of the immobilized GOx in the following temperature cycles.

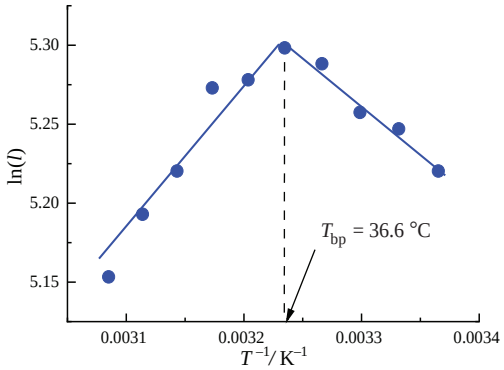

Figure 2 The temperature dependence (in the Arrhenius' coordinates) of the electrochemical responses of the SPE-MnO_2/P(NIPAM-*co*-APMA)/GOx construct measured on the addition of 2 mM of β-D-glucose solution in 50 mM HEPES/30 mM KCl (pH 7.5).

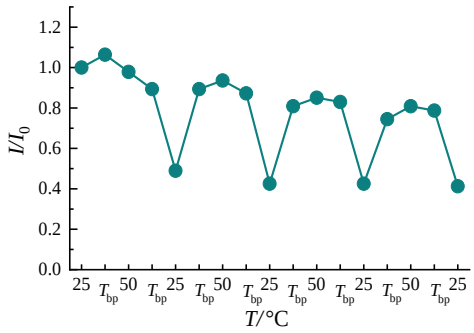

Figure 3 Evolution of the electrochemical responses of the SPE-MnO_2/P(NIPAM-*co*-APMA)/GOx constructs measured on the addition of 2 mM of β-D-glucose solution in 50 mM HEPES/30 mM KCl (pH 7.5) upon repeated temperature cycling 25 °C → T_{bp} → 50 °C → T_{bp}→ 25 °C. The electrochemical responses were normalized by the first measurement.

Thus, we highlight herein that the P(NIPAM-*co*-APMA)/GOx films can be easily fabricated onto graphite substrates (highly oriented pyrolytic graphite or graphite-based screen printed electrodes) *via* a two-stage procedure. The microgel–enzyme films were demonstrated to possess a prominent thermoresponsive behavior. Within the fabricated constructs, the microgels are strongly attached to the surface and do not show desorption upon swelling–deswelling under temperature changes. At the same time, enzyme globules loaded into the adsorbed microgel are labile and a part of them can release upon variations in temperature. The activity of the enzyme immobilized into such microgel films appears to be (reversibly) regulated by temperature-induced transformations (deswelling–swelling) of the polymer (microgel) matrix and this could be exploited for engineering of 'smart' biosensor systems.

This work was supported by the Russian Science Foundation (RSF) within the project no. 22-24-00424. The AFM measurements were carried out with the use of the atomic force microscope Asylum MFP-3D-SA (Asylum Research, Santa Barbara, CA, USA) obtained within the M. V. Lomonosov Moscow State University Program of Development. We are grateful to Dr. M. Brugnoni (Institute of Physical Chemistry II, RWTH Aachen University, Germany) for the synthesis of the P(NIPAM-*co*-APMA) microgel, which was funded by the Deutsche Forschungsgemeinschaft (DFG) within SFB 985 'Funktionelle Mikrogele und Mikrogelsysteme' (projects A3 and A6). We thank Liubov D. Pergushova for help with the preparation of the Graphical Abstract.

Online Supplementary Materials

Supplementary data associated with this article can be found in the online version at doi: 10.1016/j.mencom.2024.01.030.

References

1 R. A. Sheldon and S. van Pelt, *Chem. Soc. Rev.*, 2013, **42**, 6223.
2 U. Hanefeld, L. Gardossi and E. Magner, *Chem. Soc. Rev.*, 2009, **38**, 453.
3 A. Rodriguez-Abetxuko, D. Sánchez de Alcázar, P. Muñumer and A. Beloqui, *Front. Bioeng. Biotechnol.*, 2020, **8**, 830.
4 J. Meyer, L.-E. Meyer and S. Kara, *Eng. Life Sci.*, 2022, **22**, 165.
5 F. A. Plamper and W. Richtering, *Acc. Chem. Res.*, 2017, **50**, 131.
6 G. Agrawal and R. Agrawal, *Small*, 2018, **14**, 1801724.
7 M. Karg, A. Pich, T. Hellweg, T. Hoare, L. A. Lyon, J. J. Crassous, D. Suzuki, R. A. Gumerov, S. Schneider, I. I. Potemkin and W. Richtering, *Langmuir*, 2019, **35**, 6231.

8 J. Brijitta and P. Schurtenberger, *Curr. Opin. Colloid Interface Sci.*, 2019, **40**, 87.
9 S. Kumari, M. Avais and S. Chattopadhyay, *ACS Appl. Polym. Mater.*, 2023, **5**, 1626.
10 K. Marcisz, M. Karbarz and Z. Stojek, *Electrochem. Sci. Adv.*, 2022, **2**, e2100162.
11 L. V. Sigolaeva, S. Yu. Gladyr, A. P. H. Gelissen, O. Mergel, D. V. Pergushov, I. N. Kurochkin, F. A. Plamper and W. Richtering, *Biomacromolecules*, 2014, **15**, 3735.
12 L. V. Sigolaeva, O. Mergel, E. G. Evtushenko, S. Yu. Gladyr, A. P. H. Gelissen, D. V. Pergushov, I. N. Kurochkin, F. A. Plamper and W. Richtering, *Langmuir*, 2015, **31**, 13029.
13 L. V. Sigolaeva, S. Yu. Gladyr, O. Mergel, A. P. H. Gelissen, M. Noyong, U. Simon, D. V. Pergushov, I. N. Kurochkin, F. A. Plamper and W. Richtering, *Anal. Chem.*, 2017, **89**, 6091.
14 L. V. Sigolaeva, D. V. Pergushov, M. Oelmann, S. Schwarz, M. Brugnoni, I. N. Kurochkin, F. A. Plamper, A. Fery and W. Richtering, *Polymers*, 2018, **10**, 791.
15 L. V. Sigolaeva, D. V. Pergushov, S. Yu. Gladyr, I. N. Kurochkin and W. Richtering, *Adv. Mater. Interfaces*, 2022, **9**, 2200310.
16 L. V. Sigolaeva, A. A. Shalybkova, T. Z. Sharifullin and D. V. Pergushov, *Micromachines*, 2023, **14**, 1629.
17 L. V. Sigolaeva, O. V. Efremova and D. V. Pergushov, *Mendeleev Commun.*, 2023, **33**, 559.
18 V. Aseyev, H. Tenhu and F. M. Winnik, *Adv. Polym. Sci.*, 2011, **242**, 29.
19 O. Mergel, A. P. H. Gelissen, P. Wünnemann, A. Böker, U. Simon and F. A. Plamper, *J. Phys. Chem. C*, 2014, **118**, 26199.
20 S. Wellert, Y. Hertle, M. Richter, M. Medebach, D. Magerl, W. Wang, B. Demé, A. Radulescu, P. Müller-Buschbaum, T. Hellweg and R. von Klitzing, *Langmuir*, 2014, **30**, 7168.
21 S. Schmidt, T. Hellweg and R. von Klitzing, *Langmuir*, 2008, **24**, 12595.
22 S. Hofl, L. Zitzler, T. Hellweg, S. Herminghaus and F. Mugele, *Polymer*, 2007, **48**, 245.
23 M. Horecha, V. Senkovskyy, K. Schneider, A. Kiriy and M. Stamm, *Colloid Polym. Sci.*, 2011, **289**, 603.
24 A. Burmistrova and R. von Klitzing, *J. Mater. Chem.*, 2010, **20**, 3502.
25 E. A. Dontsova, Y. S. Zeifman, I. A. Budashov, A. V. Eremenko, S. L. Kalnov and I. N. Kurochkin, *Sens. Actuators, B*, 2011, **159**, 261.

Received: 9th October 2023; Com. 23/7265